

High-Throughput Biochemical Kinase Selectivity Assays: Panel Development and Screening Applications

AMY CARD, CHRIS CALDWELL, HYUNSUK MIN, BINA LOKCHANDER, HUALIN XI,
SIMONE SCIABOLA, AJITH V. KAMATH, SUSAN L. CLUGSTON, WILLIAM R. TSCHANTZ,
LEYU WANG, and DEBORAH J. MOSHINSKY

Kinases represent attractive targets for drug discovery. Eight small-molecule kinase inhibitors are currently marketed in the area of oncology, and numerous others are in clinical trials. Characterization of the selectivity profiles of these compounds is important to target appropriate patient populations and to reduce the potential of toxicity due to off-target effects. The authors describe the development, validation, and utilization of a biochemical kinase assay panel for the selectivity profiling of inhibitors. The panel was developed as 29 radiometric Flashplate™ assays, and then an initial 13 were transitioned to a nonradiometric Caliper mobility shift assay format. Generation of high-quality data from the panel is detailed along with a comparison of the assay formats. Both assay technologies were found to be suitable for panel screening, but mobility shift assays yielded higher data quality. The selectivity data generated here should be useful in computational modeling and help facilitate, in conjunction with sequence and structural information, the rational design of inhibitors with well-defined selectivity profiles. (*Journal of Biomolecular Screening* 2009:31-42)

Key words: kinase, panel, screening, profiling, mobility shift assay

INTRODUCTION

KINASES REPRESENT A LARGE CLASS of potential drug targets, a number of which have been heavily pursued by the pharmaceutical industry in recent years. More than 500 protein kinases have been identified, and many are linked to disease processes.¹ Eight small-molecule protein kinase inhibitors are currently on the market in the United States, including sunitinib, which was launched in 2006 for the treatment of gastrointestinal stromal tumors (GISTs) and advanced kidney cancer (renal cell carcinoma [RCC]).² All of these marketed compounds are anticancer agents, but numerous others are currently in clinical trials for oncology and nononcology indications.³ As the applications for kinase inhibitors expand beyond oncology to other diseases requiring more chronic treatments, characterizing their selectivity profiles increases in importance to reduce the potential of adverse side effects. A number of the marketed inhibitors for oncology have also been associated with toxicities from off-target effects, despite the fact that their safety profiles are generally good.⁴ Overall, information from

selectivity profiling can assist in the selection of optimized lead compounds that avoid targeting kinases implicated in toxic events.

As knowledge surrounding the molecular basis of disease continues to grow, the potential to improve efficacy of targeted therapy expands as well.⁵ A demonstration of this lies with the example of anti-epidermal growth factor receptor (EGFR) therapy and non-small cell lung cancer (NSCLC) (reviewed in Baselga⁶). Erlotinib and gefitinib, 2 agents that target EGFR, were found to be modestly effective against NSCLC in clinical trials with unselected patient populations.^{7,8} Specific subsets of patients in these trials were identified that had a better response to the therapy, and subsequently, correlations were made between positive response and mutations in EGFR.^{9,10} This illustrates nicely how an understanding of disease mechanisms and information on drug targets can combine for more efficacious treatments. The prospect of rationally designing molecules to inhibit multiple specific targets also exists—for example, to increase efficacy in complex disease processes and/or to overcome drug resistance.⁵ This will likely involve an intricate balance of inhibiting relevant targets and avoiding those associated with toxicity. Sunitinib and sorafenib are currently marketed compounds that are considered to be multitargeted kinase inhibitors,^{11,12} but much work still needs to be done in the field to more fully define disease pathways, favorable combinations of targets to inhibit, and mechanisms of toxicity for the design of optimal therapeutics.¹³

Pfizer Research Technology Center, Cambridge, Massachusetts.

Received Apr 23, 2008, and in revised form Aug 26, 2008. Accepted for publication Aug 30, 2008.

Journal of Biomolecular Screening 14(1); 2009
DOI: 10.1177/1087057108326663

Selectivity of small molecules can be assessed using a variety of methodologies (reviewed in Krishnamurty and Maly¹⁴ and Luo¹⁵). As the majority of known kinase inhibitors target the adenosine triphosphate (ATP) binding site, a number of technologies that measure selectivity *in vitro* concentrate on detecting ATP-competitive compounds. One example is a binding assay using phage display, developed by Ambit (San Diego, CA). With this method, human kinases are expressed as T7 bacteriophage fusions. Immobilized ligands are used to capture the bacterially expressed kinases by their ATP binding sites, and unmodified test compounds are assayed for the ability to compete the kinases away from the ligand.¹⁶ This method has been successfully used to profile a number of kinase inhibitors for selectivity against panels of 119 kinases¹⁶ and 317 kinases.¹⁷ One advantage to using this technology is the large number of available kinases, but it may be best used as complementary to more functional approaches to confirm that any detected binding is physiologically relevant.

More traditionally, selectivity of compounds has been assessed using panels of biochemical kinase assays.¹⁴ Multiple vendors provide this kinase selectivity screening as a fee for service, with the number of available assays well into the hundreds.¹⁸ However, establishing and running a panel of kinase assays internally offers benefits such as throughput, cost, and flexibility. In this article, we describe the development and execution of a 29-kinase assay panel in a radiometric assay format and the conversion of 13 assays to a nonradiometric mobility shift format. The 29 kinases include representatives of all the major branches of the kinome¹ in an attempt to capture the most diversity possible. Assay development and high-throughput screening (HTS) are detailed with a focus on obtaining high-quality data from the panel, along with a comparison of assay formats. Use of this panel to assess the selectivity of kinase inhibitors should complement other technologies in allowing for the design of molecules with well-defined selectivity profiles.

MATERIALS AND METHODS

Kinase production, characterization, and assay optimization

Eleven kinases were purchased from Upstate (Millipore, Billerica, MA): 3 as N-terminal GST tagged (CHK1, FGFR1, and ERK2), 7 as N-terminal HIS (GSK3 β , LCK, ABL, SRC, PDK1, SGK, and MET), and 1 as N-terminal HIS and GST (CK2). Three kinases were purchased from Invitrogen (Carlsbad, CA): 1 as an N-terminal HIS tagged (CDK2 plus N-terminal HIS CyclinA), 1 C-terminal HIS (NEK2), and 1 untagged (PKC β II). EGFR was purchased from Cell Signaling Technology (Danvers, MA) as N-terminal HIS and GST tagged. Fourteen kinases were expressed and purified internally: 11 N-terminal GST (PKA, p38 α , MK2, PAK4, TAOK3, TRK-A, INSR, VEGFR-2, AKT1, JAK3, and MASK), 2 N-terminal HIS (IKK β and AURA), and 1 N-terminal FLAG tagged (IKKi).

All kinases were of human origin with the exception of IKK β , which was from rat.

Internally generated GST-tagged proteins were purified using a Tris buffer system. Subsequent chromatographic steps were used in some cases to further purify the kinase (e.g., ion exchange, heparin). For HIS-tagged proteins, standard purification was followed by a Q ion exchange chromatography step. Purity and identity were verified by Western blotting using a specific antibody (if available), N-terminal sequencing, mass spectroscopy, and sodium dodecyl sulfate–polyacrylamide gel electrophoresis (SDS-PAGE). Typical purity for all proteins was >90%.

Optimization of radiometric assays with respect to activity, specific peptide substrate identification, reaction buffer conditions, and kinetic characterization of the kinases was performed using a coupled nicotinamide adenine dinucleotide (NADH) spectrophotometric assay.¹⁹ Caliper assays were optimized in a similar manner but using the mobility shift assay format. Peptide substrates for each assay were found by using published sequences or an internal peptide library. Reaction buffers were generally uniform to facilitate running the assays together in the panel. Buffers typically consisted of HEPES, optimal divalent cation concentration (Mg²⁺, Mn²⁺, or both), detergent (Brij-35), and dithiothreitol (DTT). For the CK2 assay, 150 mM NaCl was also included in the reaction buffer, and for PKC β II, 60 μ M CaCl₂ was added in addition to mixed micelles, consisting of 10 μ g/mL phosphatidylserine (PS) and 50 ng/mL phorbol 12-myristate 13-acetate (PMA). A number of kinases also required a preincubation with ATP or ATP plus peptide substrate to be fully activated before use in the reactions.

Kinase panel screening and compounds

All assays were performed in 384-well polypropylene assay plates. Five μ L of 5 \times concentration compound in 3.75% DMSO was first added to the plates; 10 μ L of 2.5 \times enzyme in 1.25 \times kinase buffer was added, followed by a 15-min preincubation at room temperature; and 10 μ L of a 2.5 \times mixture of peptide substrate and ATP in 1.25 \times kinase buffer was added to initiate the reaction. Each assay was run at the apparent K_m ($K_{m,app}$) concentration of ATP and at a fixed low concentration of peptide (typically 6 μ M for radiometric assays and 1.5 μ M for mobility shift assays), with an incubation time previously determined to be within the linear reaction range. Reactions were stopped by the addition of EDTA to a final concentration of 20 mM. For percent inhibition screening, compounds were tested in duplicate at both 10 μ M and 1 μ M. For IC₅₀ measurements, 11-point dose-response curves were done starting at 30 μ M, with 2.5 \times dilutions. Each plate included 16 full-activity control wells with no compound along with 16 no-reaction controls in which 20 mM EDTA was added before substrate.

For radiometric assays, tracer amounts of gamma ³³P-labeled ATP were included in the reaction. After reactions were

stopped, 25 μL was transferred to PerkinElmer (Waltham, MA) FlashplatesTM. Plates were then washed with 50 mM HEPES, soaked for 1 h with 500- μM unlabeled ATP, and rewashed before reading in a TopCount. For mobility shift assays, after the reactions were stopped, the plates were read on a Caliper LC3000 using a 12-sipper chip and separation conditions that were optimized for each kinase. Product-to-sum ratios, indicative of percent conversion from substrate to product, were taken as the assay signal. For each assay, 10% to 30% conversion was targeted as optimal for reproducible screening results. Specified compounds were purchased from Biomol International (Plymouth Meeting, PA). Other compounds screened were part of Pfizer's internal compound collection (Pfizer, New York).

Data analysis

Percent inhibition values were calculated relative to full- and no-activity controls in the following way: $[(F - S)/(F - N)] * 100\%$, where F = average signal for full-activity controls, S = signal for sample, and N = average signal for no-activity controls. IC_{50} values were calculated from dose-response curves using JavaFitter software. Correlation plots were generated and assay development data were fit using GraphPad Prism software. Heat maps of percent inhibition activity were created using Spotfire DecisionSite.

For estimated IC_{50} calculations from percent inhibition values, data transformation was first done by applying the following equation²⁰: $\text{IC}_{50} = [(100 - \text{percent inhibition at C})/\text{percent inhibition at C}] * C$, where C is the tested compound concentration. Ninety-nine percent inhibition was used for experimental values $>99\%$, and 5% was used for values $<5\%$. This created upper and lower limits of 10 nM and 190 μM for calculated IC_{50} values, or 8 and 3.7 as the $-(\log \text{IC}_{50})$, respectively, as presented later in **Figure 6**. In cases where the percent inhibition was $>99\%$ at the 10- μM testing concentration, results from 1 μM were used. Conversely, when percent inhibition was $<5\%$ at the 1- μM testing concentration, results from 10 μM were used. When percent inhibitions were between 5% and 99% at the 1- μM testing concentration, the averages of calculated IC_{50} s from 1 and 10 μM were used.

RESULTS

Kinase selectivity panel development and screening—radiometric format

As a first step in the establishment of a selectivity screening panel, an appropriate assay platform was chosen. Ideally, a uniform high-throughput format should be used for all assays to facilitate the testing of large numbers of compounds. PerkinElmer's FlashplateTM technology, in which 384-well plates are coated with scintillant and streptavidin, represents a

format that is conducive to panel screening. Provided that the kinases in question can phosphorylate a biotinylated peptide substrate, this methodology should work for any given assay. It is also based on the "gold-standard" method of radiometric incorporation of ^{33}P from the gamma position of ATP onto a peptide substrate and detection by scintillation counting, without the need for antibodies. Because the biotinylated peptide is captured on the plates, wells can also be washed to ensure detection with less active kinases.

Twenty-nine assays were developed using the FlashplateTM format by performing enzyme titrations, time courses, ATP $K_{m,app}$ determinations, and reference inhibitor IC_{50} measurements. Assay development data for 1 kinase (ABL) are shown in **Figure 1**. A summary of the ATP $K_{m,app}$ values, required enzyme concentration for each assay, and peptide sequence information is also given in **Table 1A**. Note that some assays (namely, IKK β , MET, p38 α , and VEGFR-2) required the relatively high enzyme concentration of >50 nM for the assay. This could be due to a high percentage of inactive enzyme in the protein preparation, a nonoptimal peptide substrate sequence or buffer, and/or low intrinsic activity of the kinase. These assays are inherently less sensitive than those using lower enzyme concentrations, as the lowest measurable IC_{50} will be physically bound by a minimum value of half the active enzyme concentration, assuming 1:1 binding of enzyme and inhibitor (i.e., an assay with a 100 nM active enzyme concentration could only yield a theoretical minimum of a 50 nM IC_{50} value, no matter how potent the compound).

The 29 kinase assays were collectively used to screen 6 commonly used commercially available kinase inhibitors at a single concentration in duplicate using a partially automated workstation approach. Because the intended use of the assays was predominantly to determine the degree of inhibition by ATP competitive compounds, they were each screened at the $K_{m,app}$ concentration of ATP and a set low concentration of peptide. The percent inhibition of each compound relative to the no-compound control is given in **Table 2**, and a heat map visual representation of the data is shown in **Figure 2**. A signal-to-background ratio of at least 10 was targeted for reproducible screening results, and Z' values for each of the assays were greater than or equal to 0.6. All data also passed the quality control measures that were established to ensure high-quality data (see below).

Panel development in the mobility shift assay format

Because of the environmental and safety concerns associated with using radioisotopes, a nonradioactive assay format was investigated for use in the kinase screening panel. Mobility shift assays were developed for 13 of the 29 kinases using the Caliper LC3000 "off-chip" methodology, with the intention of eventually converting the entire panel to this format. Kinase assays were performed in 384-well plates using fluorescently

Table 1. ATP $K_{m,app}$ Values and Required Enzyme Concentrations for Each Kinase Assay in (A) Radiometric and (B) Mobility Shift Assay Formats

Kinase	(A) Radiometric Assay			(B) Mobility Shift Assay		
	ATP $K_{m,app}$ (μ M)	Enzyme Concentration (nM)	Peptide Sequence ^a	ATP $K_{m,app}$ (μ M)	Enzyme Concentration (nM)	Peptide Sequence ^b
ABL	17 \pm 8	1	EAIYAAPF AKKK	11 \pm 2	0.6	EAIYAAPFAKKK
AKT1	50 \pm 12	12.5	GRPRTSSF AEG	43 \pm 2	0.8	GRPRTSSFAEG
AURA	10 \pm 3	4	LRRASLG	8 \pm 0.7	3	LRRASLG
CDK2/CycA	37 \pm 12	2.5	PKTPKKAK KL			
CHK1	77 \pm 9	15	KKKVSRSG LYRSPSMP ENLNRPR			
CK2	11 \pm 4	5	RRRDDSD DD			
EGFR	4 \pm 0.5	7	EEEEYFELV			
ERK2	22 \pm 7	20	IPTSPITTT YFFFKKK			
FGFR1	191 \pm 75	6.25	KKKSPGEY VNIEFG	185 \pm 11	6	KKSRGDYMTMQIG
GSK3 β	8 \pm 3	6.25	YRRAAVPP SPSLSRHS SPHQ(pS)E DEEE			
IKK β	0.3 \pm 0.06	100	GLKKERLL DDRHDSGL DSMKDEE			
IKKi	0.4 \pm 0.05	8	GLKKERLL DDRHDSGL DSMKDEE			
INSR	42 \pm 15	5	KKSRGDYMTMQIG	64 \pm 6	1	KKSRGDYMTMQIG
JAK3	6 \pm 1	3	GGEIEEYF ELVKKKK			
LCK	55 \pm 12	12.5	KVEKIGEG TYGVVYK	13 \pm 2	0.3	EGIYGVFLKKK
MK2	7 \pm 1	1.25	KKKALSRQ LSVAA	5 \pm 0.4	0.3	KKLRRTLSVA
MASK	53 \pm 4	10	KRTLRRKR TLRRKRTL RR			
MET	29 \pm 10	50	Ac-RDMYD KEYYSVHNK	17 \pm 3	7.5	EAIYAAPFAKKK
NEK2	3 \pm 0.6	2	RFRRSRRMI			
PAK4	6 \pm 0.6	5	RRKSLVG (pT)PYWMAPE			
PDK1	3 \pm 1	30	KTFCGTPE YLAPEVRR EPRILSEE EQEMFRDF DYIADWC			
PKA	20 \pm 9	0.25	LRRASLG	4 \pm 1	0.07	LRRASLG
PKC β II	94 \pm 14	0.25	RFARKGSL RQKNV			
P38 α	126 \pm 40	100	KRELVEPL TPSGEAPN QALLR	194 \pm 24	5	IPTSPITTTYFFFKKK

(continued)

Kinase Biochemical Assay Panel Screening

Table 1. (continued)

Kinase	(A) Radiometric Assay			(B) Mobility Shift Assay		
	ATP $K_{m,app}$ (μ M)	Enzyme Concentration (nM)	Peptide Sequence ^a	ATP $K_{m,app}$ (μ M)	Enzyme Concentration (nM)	Peptide Sequence ^b
SGK	59 \pm 5	2	GRPRTSSF AEG	54 \pm 3	0.25	GRPRTSSFAEG
SRC	25 \pm 8	3	EGIYGVLV KKK	15 \pm 2	0.35	EGIYGVLVKKK
TAOK3	15 \pm 6	40	VDGKEIYN TIRRK			
TRK-A	77 \pm 16	40	RRRAAAEE IYGEI			
VEGFR-2	145 \pm 46	50	KKKSPGEY VNIEFG	150 \pm 17	30	IPTSPITTTYFFFKKK

$K_{m,app}$ values are averages plus or minus standard deviation for 3 to 6 independent determinations; enzyme concentrations are the minimum required to yield a robust assay signal at the $K_{m,app}$ concentration of adenosine triphosphate (ATP) within the linear range (normally 60 min).

a. Peptides for the radiometric assay were biotinylated on their N-termini followed by a 6-carbon linker.

b. Peptides for the mobility shift assay were labeled with fluorescein on their N-termini.

labeled peptide substrate, and the amount of phosphorylated product was quantified following electrophoretic separation in the chip. This assay format is expected to yield superior data quality to radiometric assays because it represents a direct quantification of percent conversion to product, without artifacts associated with indirect measurements. Assay development was performed as indicated for the radiometric assays. ATP $K_{m,app}$ values, required enzyme concentrations, and peptide sequences for each are summarized in **Table 1B**. Note that initial mobility shift assay conditions for the remaining 16 kinase assays were also successfully determined with the expectation that these can be converted from the radiometric format as well (data not shown). Z' values for the mobility shift assays typically ranged from 0.8 to 0.9.

Throughput for the mobility shift assay was similar to that of the radiometric format, as kinase reactions were performed in the same manner for both. Given that compounds were tested in 384-well plates (minus 48 control wells) at 2 concentrations in duplicate, 84 samples can be screened per plate. Assuming 3 compound plates per kinase, one could screen 252 compounds against 29 kinases (87 total plates) for percent inhibition in 1 to 2 days. Read time on the LC3000 ranged from 10 to 35 min, depending on the assay. Average read time was approximately 20 min a plate. For the radiometric assays, read time was approximately 8 min a plate.

General panel screening, validation, and quality control

A number of validation experiments were performed and controls put in place to ensure that high-quality data were

generated from the kinase assay panel. In general, some important overall considerations when running the panel are that (1) reagent additions and enzymatic reactions proceed as expected, (2) single-concentration percent inhibition values approximate the value generated from full IC_{50} curves, (3) data are reproducible between replicates and on different days, and (4) similar results are obtained with all assay formats in use. To address these points, we performed reference IC_{50} controls for each kinase in every run, and reproducibility/comparison experiments were conducted. Plate visualization software was also used to inspect individual well percent inhibition values and look for trends indicative of liquid handling issues.

Consistency of reference IC_{50} values for each kinase is an essential control for running a kinase panel. Variability in the results can be indicative of altered test conditions such as increased ATP, incubation time, and so on, and therefore data should only be acceptable when control IC_{50} s vary less than approximately 3-fold between different runs of any given assay. **Figure 3** depicts IC_{50} curves for 3 control compounds in the AURA assays in both the Caliper and Flashplate™ assay formats. IC_{50} values are also indicated below the curves to show the consistency of values between separate assay runs.

To test the reproducibility of results from screening, we compared percent inhibition values for selected compounds between replicate samples and also on different days. Two hundred compounds with varying potencies toward ABL were tested at 1 μ M in duplicate in both the ABL radiometric and mobility shift assays. Values from 1 replicate were plotted against those from the other replicate from both assay formats, and the graphs are presented in **Figure 4A, B**. To investigate

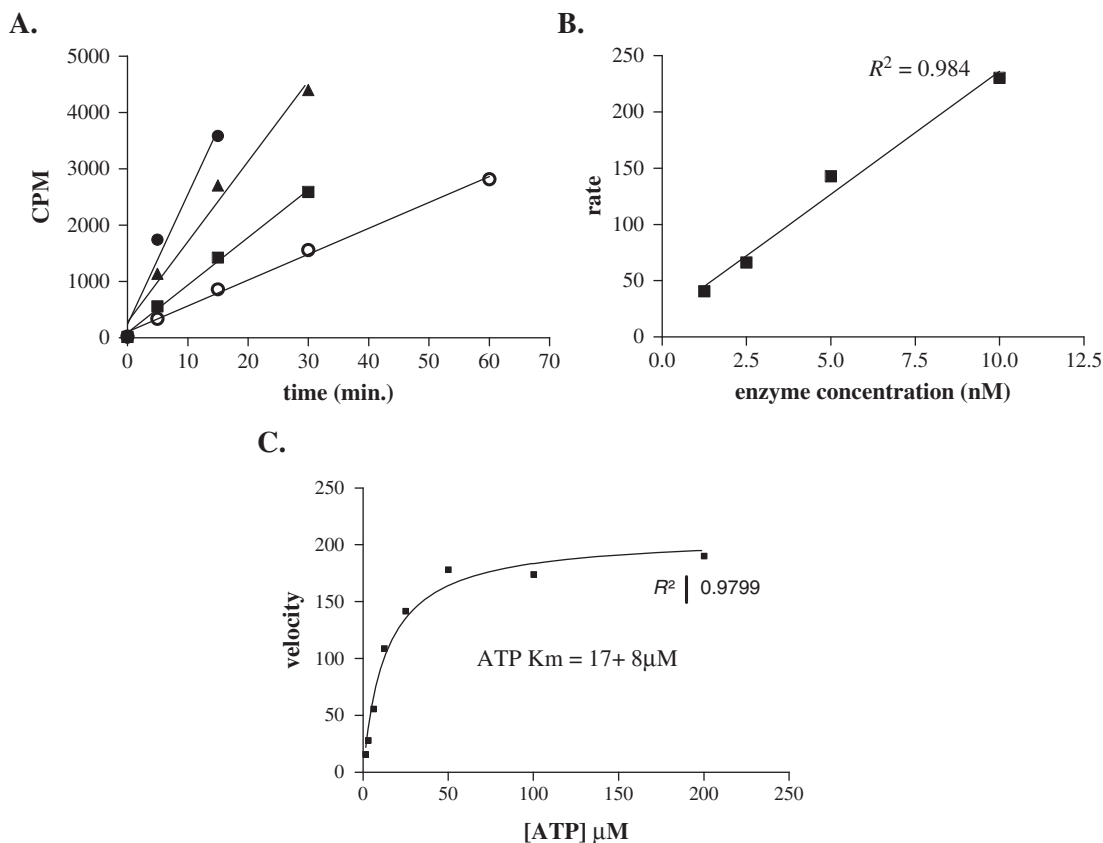


FIG. 1. Radiometric assay development data for ABL kinase. (A) Radiometric counts per minute (CPM) measurements as a function of time for 10 nM (closed circles), 5 nM (triangles), 2.5 nM (squares), and 1.25 nM enzyme (open circles). (B) Rate versus enzyme concentration plot. (C) Rate versus adenosine triphosphate (ATP) concentration plot for ATP $K_{m,app}$ determination. This plot depicts representative data from 4 $K_{m,app}$ determinations, and the value is the average plus or minus the standard deviation of the 4.

the reproducibility of data in independent experiments, 170 compounds in the ABL mobility shift assay were also tested at 1 μM in duplicate on 2 different days. Average percent inhibition values from 1 day were plotted against those from the other, and the result is given in **Figure 4C**. R^2 values for each of the 3 plots are also shown to indicate the correlation between the measured values.

Because the assay panel was being run using 2 different formats, it was important to determine whether data obtained from either are similar. To investigate this, we tested a number of compounds for percent inhibition at 1 μM in both formats against a given kinase, and the data were compared. **Figure 5** depicts plots of percent inhibition values generated from the mobility shift assay format versus those from the radiometric format for 3 kinase assays—namely, ABL, PKA, and LCK. High R^2 values for each plot indicate that the data are highly correlative.

After a large number of compounds had been tested against each assay in the panel for both percent inhibition and IC_{50} , it was possible to evaluate overall data quality and consistency by correlating measured IC_{50} s to calculated IC_{50} s from percent

inhibition values. For running the panel, the standard methodology for percent inhibition screening was to test each sample in duplicate at both the 1 μM and 10 μM concentration. The rationale behind this was to ensure productive measurements for a wide range of inhibitor potencies. Guidelines were created for calculating estimated IC_{50} s from single concentration screening, whereby (1) percent inhibition values at the lower screening concentration were used for compounds yielding >99% inhibition at the higher concentration, (2) values at the higher screening concentration were used for compounds yielding <5% inhibition at the lower screening concentration, and (3) an average of the estimated IC_{50} values was calculated when percent inhibition values were between 5% and 99%. With this in mind, estimated IC_{50} s were calculated for approximately 7500 compound/assay combinations from percent inhibition screening results and plotted against values measured from full 11-point dose-response curves. The graph depicting these results is given in **Figure 6**, including the R^2 value from a linear fit of the data. Compounds that fall within the triangle at the lower right corner of the plot were over 10-fold more potent in IC_{50} measurements compared with percent inhibition. Those in

Kinase Biochemical Assay Panel Screening

Table 2. Panel Kinase Inhibition for 6 Compounds

Kinase	<i>H-8</i> (10 μ M)	<i>PP1</i> (1 μ M)	<i>Roscovitine</i> (1 μ M)	<i>SB-203580</i> (1 μ M)	<i>SP 600125</i> (1 μ M)	<i>Staurosporine</i> (1 μ M)
ABL	8 \pm 3	85 \pm 0	9 \pm 2	3 \pm 5	37 \pm 1	98 \pm 1
AKT1	74 \pm 2	0 \pm 5	-8 \pm 2	1 \pm 5	7 \pm 6	101 \pm 0
AURA	2 \pm 3	3 \pm 7	-1 \pm 3	-9 \pm 6	81 \pm 0	102 \pm 0
CDK2/cyclin A	8 \pm 1	0 \pm 9	75 \pm 3	-6 \pm 1	31 \pm 4	103 \pm 1
CHK1	-3 \pm 1	-14 \pm 6	-13 \pm 2	-11 \pm 0	7 \pm 0	103 \pm 0
CK2	4 \pm 0	-1 \pm 3	2 \pm 5	-10 \pm 6	71 \pm 0	41 \pm 1
EGFR	1 \pm 1	97 \pm 1	5 \pm 0	81 \pm 2	18 \pm 9	101 \pm 1
FGFR1	5 \pm 0	14 \pm 0	-11 \pm 1	-7 \pm 0	37 \pm 0	102 \pm 0
GSK3 β	7 \pm 1	-2 \pm 2	-5 \pm 7	53 \pm 1	16 \pm 9	104 \pm 1
IKK β	0 \pm 3	-5 \pm 15	-4 \pm 0	-10 \pm 2	22 \pm 1	65 \pm 2
IKKi	-1 \pm 5	-10 \pm 6	1 \pm 2	-8 \pm 1	30 \pm 9	99 \pm 0
INSR	-3 \pm 6	0 \pm 6	1 \pm 1	1 \pm 2	30 \pm 1	102 \pm 1
JAK3	-8 \pm 2	-16 \pm 0	-3 \pm 8	-11 \pm 9	82 \pm 3	106 \pm 0
LCK	-5 \pm 2	87 \pm 1	-10 \pm 5	7 \pm 7	14 \pm 0	102 \pm 1
ERK2	13 \pm 4	14 \pm 6	19 \pm 5	12 \pm 0	22 \pm 3	63 \pm 1
MK2	-9 \pm 2	-4 \pm 1	-11 \pm 4	-17 \pm 10	-11 \pm 0	85 \pm 0
MASK	2 \pm 4	-6 \pm 5	-2 \pm 4	-16 \pm 2	24 \pm 10	83 \pm 16
MET	-11 \pm 9	-11 \pm 1	-3 \pm 6	-7 \pm 2	11 \pm 1	90 \pm 0
NEK2	-7 \pm 6	-7 \pm 3	-7 \pm 3	-6 \pm 8	-5 \pm 0.2	64 \pm 2
PAK4	2 \pm 4	3 \pm 8	3 \pm 1	7 \pm 4	36 \pm 2	102 \pm 0
PDK1	-2 \pm 4	-17 \pm 8	-13 \pm 2	-4 \pm 14	40 \pm 0	106 \pm 0
PKA	96 \pm 2	29 \pm 5	6 \pm 1	18 \pm 3	33 \pm 9	101 \pm 0
PKC β II	18 \pm 2	14 \pm 3	8 \pm 2	24 \pm 1	16 \pm 1	103 \pm 0
p38 α	11 \pm 2	41 \pm 5	5 \pm 2	96 \pm 0	17 \pm 9	65 \pm 2
SGK	22 \pm 6	1 \pm 6	2 \pm 4	7 \pm 1	50 \pm 0	102 \pm 0
SRC	6 \pm 9	97 \pm 1	5 \pm 3	17 \pm 4	17 \pm 5	101 \pm 1
TAOK3	13 \pm 6	6 \pm 8	4 \pm 5	16 \pm 7	36 \pm 12	106 \pm 0
TRK-A	10 \pm 6	38 \pm 2	3 \pm 1	4 \pm 3	82 \pm 1	102 \pm 0
VEGFR-2	12 \pm 2	57 \pm 6	1 \pm 4	13 \pm 3	53 \pm 0	100 \pm 1

The testing concentration is indicated below each inhibitor, and values are expressed as percent inhibition (relative to full- and no-activity controls). Values are averages of replicate measurements, and each experiment was performed in duplicate with similar results.

the dashed triangle in the upper left corner of the plot were over 10-fold less potent in IC₅₀ measurements compared with percent inhibition.

DISCUSSION

In this study, we have developed, validated, and used a panel of 29 biochemical kinase screening assays for the selectivity assessment of compounds. All were initially run in a radiometric assay format, and then a number were converted to a nonradiometric, mobility shift format. Quality control measures for running a kinase panel were also outlined, and high-quality screening data were demonstrated as measured by reproducibility (Figs. 3 and 4), a very good data correlation between the 2 different assay formats (Fig. 5), and ultimately a good correlation between measured IC₅₀s and those calculated from percent inhibition data (Fig. 6). The comparison between measured and calculated IC₅₀s also revealed that few compounds exhibited a shift of more than 10-fold in potency between percent inhibition and IC₅₀ values (1.9% of total compounds),

implying a low false-positive/negative rate with percent inhibition screening. This rate may also be vastly overestimated, as the data set used was not controlled for sources of compound, the possibility of degradation, or inhibitor solubility. Nevertheless, good practice for the confirmation of any selectivity screening result is to ensure that data are reproducible with compounds whose physical properties are well characterized.

In general, the selectivity profiles obtained here with the commonly used kinase inhibitors are similar to those reported. Roscovitine was found to be very selective toward CDK2 in the panel tested; previous reports using radiometric filter binding²¹ or a phage display binding assay¹⁷ were consistent with these results. PP1, originally reported as an SRC family inhibitor with activity against EGFR,²² was found to inhibit SRC, LCK, ABL, and EGFR with moderate activity against other kinases, including p38 α , which is consistent with earlier reports.²¹ SP 600125 inhibited a number of kinases, most notably AURA, CK2, JAK3, and TRK-A. This is in accord with the earlier panel screening study where Aurora family kinases, CK2, and

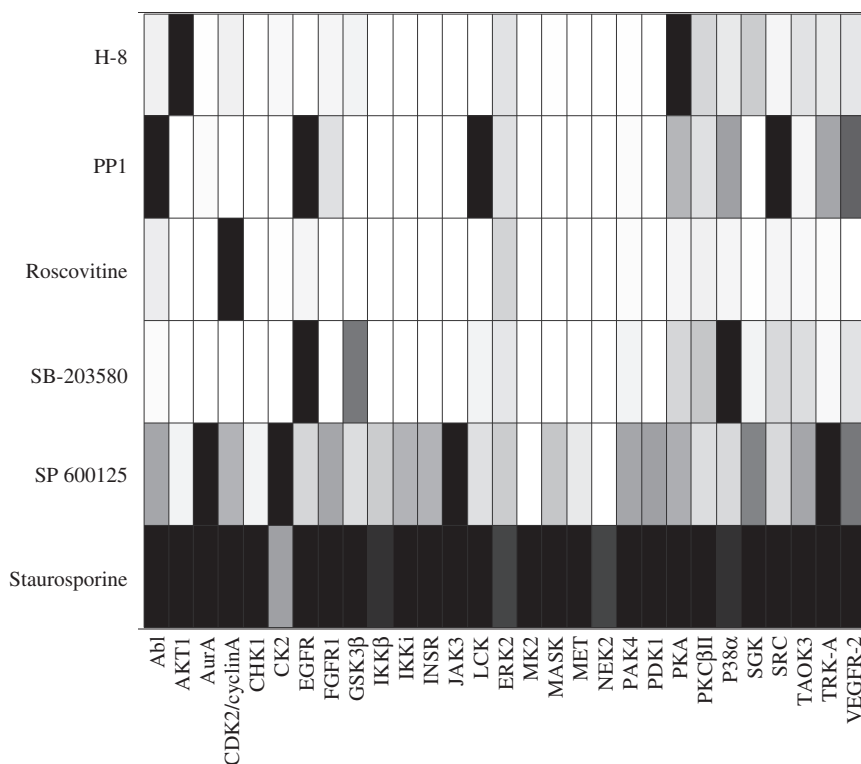


FIG. 2. Heat map representation of percent inhibition data by compounds against the kinases in the panel. Compound concentrations, number of replicates, and percent inhibition values are as indicated in **Table 2**. Color scale ranges from white (no inhibition) to black (100% inhibition).

SGK1, among others, were also inhibited.²¹ In this study, SB-203580 hit p38 α , EGFR, and, to a lesser extent, GSK3 β . This also concurs with both the activity and binding panels^{17,21} in which the specified kinases were inhibited or showed binding.

Both the radiometric (FlashplateTM) assay format and the Caliper mobility shift format were found to be suitable for biochemical kinase panel screening, but the mobility shift assays displayed some overall benefits. Logistically, compared with the radiometric format employed here, mobility shift assays were easier to perform owing to the lack of radioactivity and the fact that there are no transfer or washing steps of the plates. This was especially apparent for kinases with high ATP $K_{m,app}$ values, where a relatively large amount of radiolabeled ATP and extensive washing were required for a robust signal in the radiometric assays. Mobility shift assays worked equally well, with no wash steps, for all assays regardless of ATP concentration. A further benefit to the mobility shift assay technology in general was that on average, less enzyme was required to perform the assays. The amount of enzyme required ranged from 1.04 \times to 41.7 \times less than the amount required for the radiometric assays (**Table 1**). This not only reduces the cost to perform the assays, but increases their sensitivities as lower IC_{50} values can be measured.

With respect to data quality, mobility shift assays may be expected to yield data with less variability because they directly quantify the amount of product; this fact was supported by the data presented here. Replicate correlations using the mobility shift assay were generally better than those using the radiometric format (**Fig. 4B** vs. **4A**), especially in the lower range of inhibition. This implies that variability of results should be less with the mobility shift format, a fact supported by the smaller error bars on the IC_{50} curves shown in **Figure 3** (compare **3A** with **3B**) and that Z' values were typically higher for mobility shift assays in general (0.8 to 0.9 vs. 0.6 to 0.7). Less variability should also improve sensitivity because of better reproducibility in the lower range of inhibition. The highly reproducible data obtained here with the mobility shift assay support that seen in previous studies with kinase assays²³ and extend the findings to use in panel screening.

Excellent correlation of active compounds was found between the 2 assay formats used in this study (**Fig. 5**). This was the case for assays in which conditions and peptide substrate were the same between the formats (e.g., PKA) but also in which the peptide substrate and ATP $K_{m,app}$ differed (e.g., LCK). The relatively high degree of scatter around the origin in the LCK radiometric versus mobility shift plot (**Fig. 5C**) is

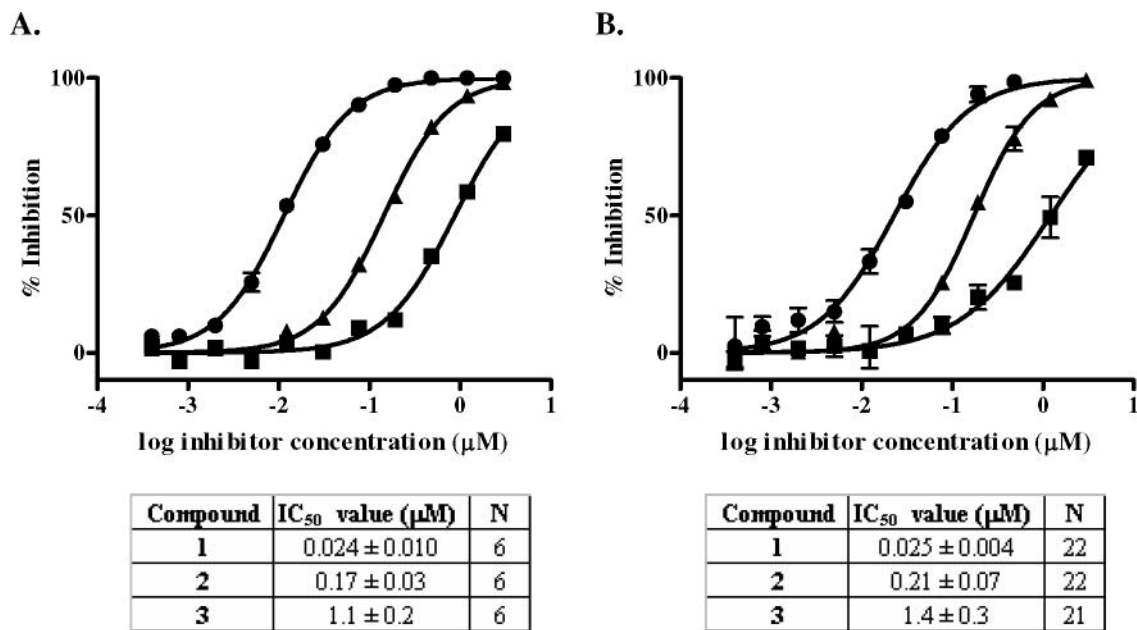


FIG. 3. Reference IC₅₀ curves for the AURA assay. (A) Mobility shift and (B) radiometric assay data for 3 reference compounds. Percent inhibition is relative to full-activity and no-activity controls, and N is the number of times the compound was tested with duplicate measurements.

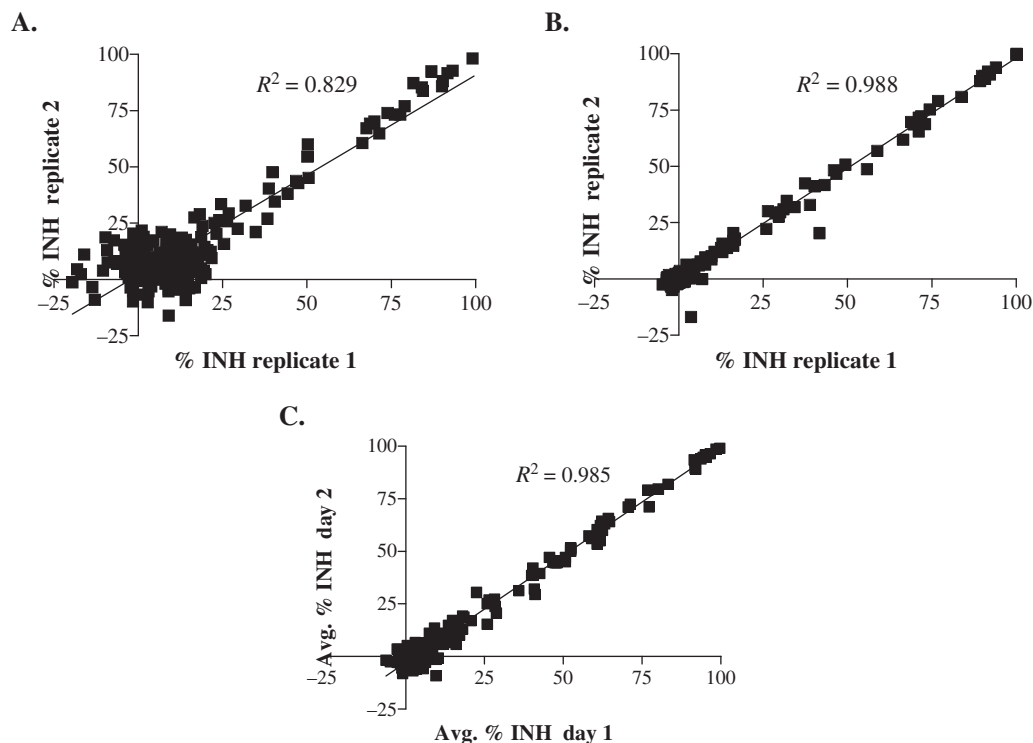


FIG. 4. Reproducibility of screening results. Plot of percent inhibition values between replicate samples for 200 compounds at 1 μM against the ABL kinase assay in (A) radiometric and (B) mobility shift assay format. (C) Variability between measurements on different days for the ABL kinase mobility shift assay is illustrated by a plot of average percent inhibition values (of duplicates at 1 μM) on day 1 versus day 2. INH, inhibition.

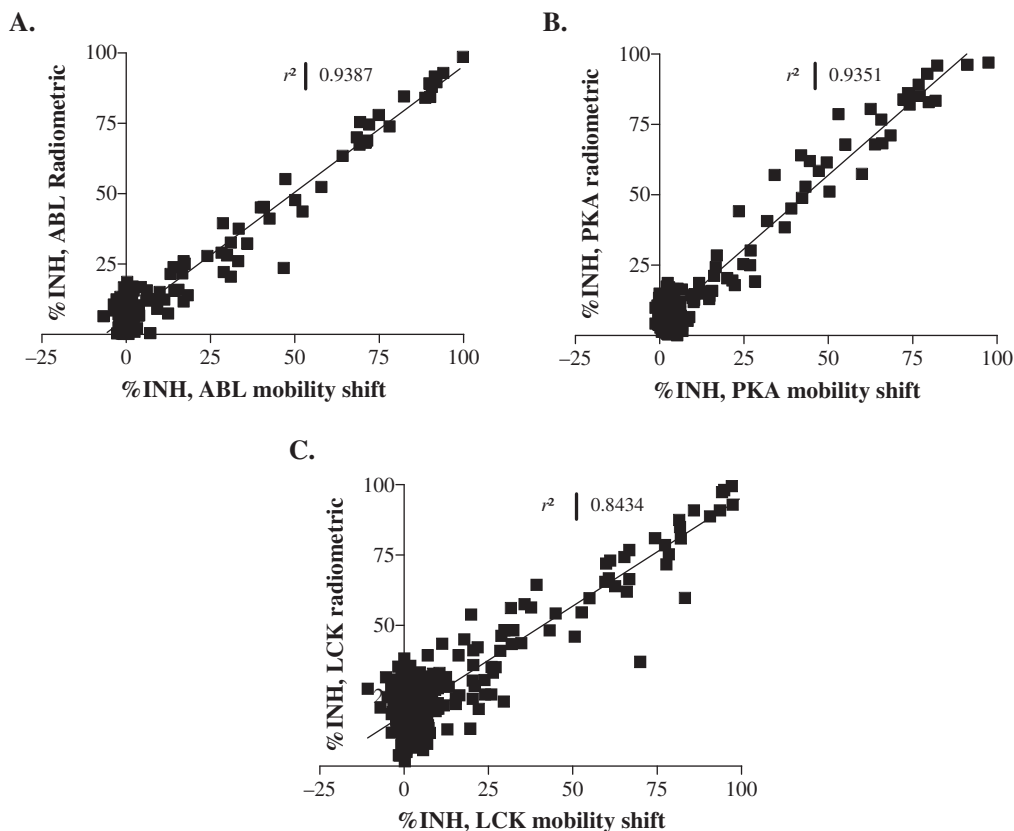


FIG. 5. Correlation of screening results between formats. Plot of percent inhibition values for 200 compounds at 1 μ M in the mobility shift assay versus radiometric assay for (A) ABL and (B) PKA. (C) Plot of percent inhibition values for 240 compounds at 1 μ M in the LCK mobility shift versus radiometric assay. INH, inhibition.

thought to occur because of the higher variability of radiometric data in the lower range of inhibition (compare **Fig. 4A** with **4B**; also discussed above). The overall data concordance using different kinase assay technologies is similar to that seen by other investigators (e.g., Schröter et al.²⁴ and Huss et al.²⁵) but disagrees with that seen in a previous study using a tyrosine kinase for HTS and comparing a scintillation proximity assay (SPA), homogeneous time-resolved fluorescence resonance energy transfer (HTR-FRET), and fluorescence polarization (FP).²⁶ Reasons for this are unknown but may include the fact that different assay formats, methodologies, and compound sources were being used. The current study also used a much smaller subset of compounds in which fluorescence or other artifacts were less likely to be of issue.

Selectivity screening data have much utility throughout the drug discovery process for kinase inhibitors. Early on, selectivity data can assist in the prioritization of series identified in HTS. Testing multiple analogs against multiple kinases can reveal structure-activity relationships (SARs) or lack thereof for kinases in the panel, thus allowing more informed decisions

about which series to pursue for a particular selectivity profile. In terms of new kinase drug discovery projects, mining selectivity data can be particularly useful for kinases that are already on the panel, allowing for a quick start on attractive chemical matter. For inhibitors that already are efficacious, more complete knowledge of their selectivity profiles can suggest new indications for their use. An illustration of this lies with the discovery that imatinib, a kinase inhibitor originally thought to be selective toward ABL and PDGFR, also inhibits c-KIT.²⁷ This discovery led to the use of imatinib in GIST, in which the activating mutation of c-KIT is common.²⁸

Selectivity data can also be used in conjunction with sequence and structural information in a chemogenomic, gene family approach for maximizing the efficiency of kinase inhibitor discovery.²⁹ Computational methodologies have been continuously advancing in an effort to model and predict selectivity, reclassify kinases based on inhibitor sensitivities, and generally understand the molecular determinants of selectivity (reviewed in Ortiz et al.³⁰ and Rockey and Elcock³¹). These approaches, partially powered by selectivity data such as that

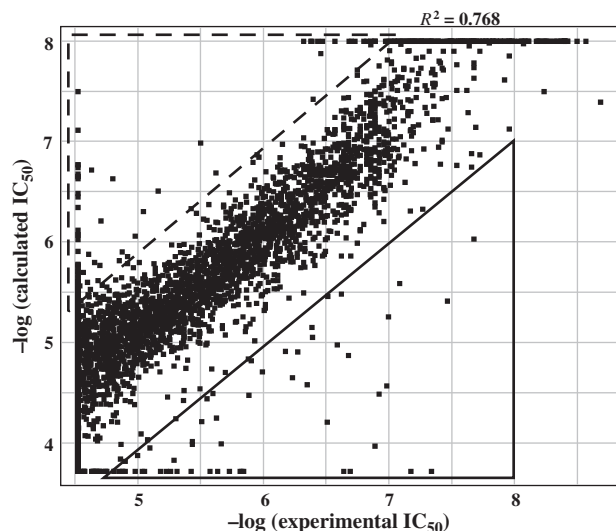


FIG. 6. Correlation of experimental IC_{50} values to those calculated from percent inhibition. Plot of experimental IC_{50} s versus those calculated from percent inhibition values. In total, 7506 data points (compound + assay combinations) are indicated on the graph. Triangles depict the approximate areas where experimental IC_{50} values were 10 or more times higher (dashed triangle) or lower (solid triangle) than those calculated from percent inhibition. Upper and lower limits for calculated IC_{50} s were 190 μ M and 10 nM (for details, see Materials and Methods). Upper and lower limits for experimental IC_{50} s were 30 μ M and 3 nM, representing the highest and lowest testing concentrations.

generated in this study, work toward the long-term goal of rationally designing compounds to have particular selectivity profiles that will maximize efficacy while minimizing adverse effects. Recently, we have used selectivity data generated here to develop quantitative SAR (QSAR) models to predict the selectivity profiles of 2 series.³²

In summary, we have developed and used a panel of biochemical kinase assays for selectivity screening of compounds. Profiles generated from the panel currently have valuable utility throughout the drug discovery process. Eventually, these data, used together with other types of selectivity results, kinase sequence and structural information, and computational input, can lead to the tailored design of molecules with particular selectivity profiles.

ACKNOWLEDGMENTS

We acknowledge the contributions of Yan Zhang, Gayatri Deshmukh, Kim Verdries, and Suzanne Jacques-O'Hagan for protein characterization and radiometric assay optimization; Caryl Lane, Rocco Coli, and Lily Yang for protein purification; D. Michael Corcoran, Ryan Navratil, and Chris Hagaman for compound handling; Sergio Rotstein, Peter

Henstock, and Ya Chen for data handling; Daniel Caffrey and Beth Lunney for panel design; Bridget Cole and Alan Cheng for data applications; Javier Farinas and Jude Dunne at Caliper Life Sciences for mobility shift assay optimization; and Cyrille Kuhn, Ralph Lambalot, and Jessie English for helpful support.

REFERENCES

- Manning G, Whyte DB, Martinez R, Hunter T, Sudarsanam S: The protein kinase complement of the human genome. *Science* 2002;298:1912-1934.
- FDA approves new treatment for gastrointestinal and kidney cancer. 2006 [Online]. Retrieved from. <http://www.fda.gov/bbs/topics/news/2006/NEW01302.html>
- <http://clinicaltrials.gov/>
- Widakowich C, de Castro G Jr, de Azambuja E, Dinh P, Awada A: Review: side effects of approved molecular targeted therapies in solid cancers. *Oncologist* 2007;12:1443-1455.
- Garber K: The second wave in kinase cancer drugs. *Nat Biotechnol* 2006;24:127-130.
- Baselga J: Targeting tyrosine kinases in cancer: the second wave. *Science* 2006;312:1175-1178.
- Shepherd FA, Rodrigues Pereira J, Ciuleanu T, Tan EH, Hirsh V, Thongprasert S, et al: Erlotinib in previously treated non-small-cell lung cancer. *N Engl J Med* 2005;353:123-132.
- Thatcher N, Chang A, Parikh P, Rodrigues Pereira J, Ciuleanu T, von Pawel J, et al: Gefitinib plus best supportive care in previously treated patients with refractory advanced non-small-cell lung cancer: results from a randomised, placebo-controlled, multicentre study (Iressa Survival Evaluation in Lung Cancer). *Lancet* 2005;366:1527-1537.
- Lynch TJ, Bell DW, Sordella R, Gurubhagavatula S, Okimoto RA, Brannigan BW, et al: Activating mutations in the epidermal growth factor receptor underlying responsiveness of non-small-cell lung cancer to gefitinib. *N Engl J Med* 2004;350:2129-2139.
- Paez JG, Janne PA, Lee JC, Tracy S, Greulich H, Gabriel S, et al: EGFR mutations in lung cancer: correlation with clinical response to gefitinib therapy. *Science* 2004;304:1497-1500.
- Ahmad T, Eisen T: Kinase inhibition with BAY 43-9006 in renal cell carcinoma. *Clin Cancer Res* 2004;10:6388S-6392S.
- O'Farrell AM, Abrams TJ, Yuen HA, Ngai TJ, Louie SG, Yee KW, et al: SU11248 is a novel FLT3 tyrosine kinase inhibitor with potent activity in vitro and in vivo. *Blood* 2003;101:3597-3605.
- Castoldi RE, Pennella G, Saturno GS, Grossi P, Brughera M, Venturi M: Assessing and managing toxicities induced by kinase inhibitors. *Curr Opin Drug Discov Devel* 2007;10:53-57.
- Krishnamurthy R, Maly DJ: Chemical genomic and proteomic methods for determining kinase inhibitor selectivity. *Comb Chem High Throughput Screen* 2007;10:652-666.
- Luo Y: Selectivity assessment of kinase inhibitors: strategies and challenges. *Curr Opin Mol Ther* 2005;7:251-255.
- Fabian MA, Biggs WH III, Treiber DK, Atteridge CE, Azimioara MD, Benedetti MG, et al: A small molecule-kinase interaction map for clinical kinase inhibitors. *Nat Biotechnol* 2005;23:329-336.
- Karaman MW, Herrgard S, Treiber DK, Gallant P, Atteridge CE, Campbell BT, et al: A quantitative analysis of kinase inhibitor selectivity. *Nat Biotechnol* 2008;26:127-132.

18. Comley J: Kinase screening and profiling: spoilt for choice. *Drug Discovery World* 2006;8:27-50.
19. Schelling P, Folkers G, Scapozza L: A spectrophotometric assay for quantitative determination of kcat of herpes simplex virus type 1 thymidine kinase substrates. *Anal Biochem* 2001;295:82-87.
20. Ekins S, Gao F, Johnson DL, Kelly KG, Meyer RD: Single point interaction screen to predict IC₅₀. 2001. Patent EP1139267.
21. Bain J, Plater L, Elliott M, Shpiro N, Hastie CJ, McLauchlan H, et al: The selectivity of protein kinase inhibitors: a further update. *Biochem J* 2007;408:297-315.
22. Hanke JH, Gardner JP, Dow RL, Changelian PS, Brissette WH, Weringer EJ, et al: Discovery of a novel, potent, and Src family-selective tyrosine kinase inhibitor: study of Lck- and FynT-dependent T cell activation. *J Biol Chem* 1996;271:695-701.
23. Dunne J, Reardon H, Trinh V, Li E, Farinas J: Comparison of on-chip and off-chip microfluidic kinase assay formats. *Assay Drug Dev Technol* 2004;2:121-129.
24. Schröter T, Minond D, Weiser A, Dao C, Habel J, Spicer T, et al: Comparison of miniaturized time-resolved fluorescence resonance energy transfer and enzyme-coupled luciferase high-throughput screening assays to discover inhibitors of Rho-kinase II (ROCK-II). *J Biomol Screen* 2008;13:17-28.
25. Huss KL, Blonigen PE, Campbell RM: Development of a Transcreeper kinase assay for protein kinase A and demonstration of concordance of data with a filter-binding assay format. *J Biomol Screen* 2007;12:578-584.
26. Sills MA, Weiss D, Pham Q, Schweitzer R, Wu X, Wu JJ: Comparison of assay technologies for a tyrosine kinase assay generates different results in high throughput screening. *J Biomol Screen* 2002;7:191-214.
27. Heinrich MC, Griffith DJ, Druker BJ, Wait CL, Ott KA, Zigler AJ: Inhibition of c-kit receptor tyrosine kinase activity by STI 571, a selective tyrosine kinase inhibitor. *Blood* 2000;96:925-932.
28. Demetri GD, von Mehren M, Blanke CD, Van den Abbeele AD, Eisenberg B, Roberts PJ, et al: Efficacy and safety of imatinib mesylate in advanced gastrointestinal stromal tumors. *N Engl J Med* 2002;347:472-480.
29. Harris CJ, Stevens AP: Chemogenomics: structuring the drug discovery process to gene families. *Drug Discov Today* 2006;11:880-888.
30. Ortiz AR, Gomez-Puertas P, Leo-Macias A, Lopez-Romero P, Lopez-Vinas E, Morreale A, et al: Computational approaches to model ligand selectivity in drug design. *Curr Top Med Chem* 2006;6:41-55.
31. Rockey WM, Elcock AH: Rapid computational identification of the targets of protein kinase inhibitors. *Curr Opin Drug Discov Devel* 2006;9:326-331.
32. Sciabola S, Stanton RV, Wittkopp S, Wildman S, Moshinsky D, Potluri S, et al: Predicting kinase selectivity profiles using Free-Wilson QSAR analysis. *J Chem Inf Model*. 2008;48:1851-1867.

Address correspondence to:

Deborah J. Moshinsky
Pfizer Research Technology Center
620 Memorial Drive
Cambridge, MA 02139

E-mail: deborah.moshinsky@pfizer.com